JOURNAL OF OPTOELECTRONICS AND ADVANCED MATERIALS Vol. 16, No. 11-12, November - December 2014, p. 1322 - 1327

High pressure phase transition and elastic behavior of europium oxide

M. GÜLER*, E. GÜLER
Hitit University, Department of Physics, 19030 Corum - Turkey

We report the questionable high pressure structural and elastic characteristics of europium oxide (EuO) up to 50 GPa with shell model potential framework by geometry optimization calculations. We determined B1→B2 phase transformation pressure of EuO as 43 GPa and a bulk modulus value as 106 GPa at zero Kelvin temperature under zero pressure. During search, we also determined the pressure dependence of typical cubic elastic constants, shear modulus, Young's modulus, elastic wave velocities, static and high frequency dielectric constants. Overall, our results show a fair agreement between experiments and competing with former theoretical findings.

(Received 7 March 2014; accepted November 13, 2014)

Keywords: EuO, High pressure, Elastic constants, Dielectric constants, Phase transition

1. Introduction

Understanding the high pressure behavior of materials is critical for finding out precious physical knowledge about the elastic characteristics of considered material. For example, high pressure investigations describe the nature of the stability, phase transformation and elastic responses of a given material [1].

Today, rare earth element based compounds are the key materials for both science and technology. In particular, these materials encountered with prominent usage progress over the past 30 years [2]. Among them, europium compounds, EuX (X = O, S, Se and Te) are of great importance. They exhibit several distinguished structural, optical, magnetic, electronic, and semiconducting properties. Several outstanding technological applications implicate the magneto-optical modulators; magnetic field activated electronic switches and addressable computer memories [3]. From EuX compounds, EuO is an exciting research issue for scientists since this oxide shows an electronic transformation at 30 GPa and a crystallographic phase transformation at 40 GPa. Therefore, much scientific effort has been devoted to clarify this challenging nature of EuO under high pressure. Experimentally, conventional techniques such as ultrasonic analyses and Brillouin spectroscopy are quite scant gauges for high pressures. Because, ultrasonic measurements are operable under few gigapascals and Brillouin spectroscopy are limited up to 25GPa. To compensate these experimental lacks, investigators accomplish computational methods beyond the pure theoretical calculations for high pressure studies. Two popular options are molecular dynamics (MD) simulations and density functional theory (DFT) computational techniques that both techniques can yield reliable findings by employing correct interatomic potentials to the computations.

Earlier reports incorporate diverse works and different results linking with the high pressure elastic behavior of EuX compounds with dissimilar interatomic potentials. In 1994, Islam and Shahdatullah [4] surveyed elastic and other properties of EuO and EuS up to 30 GPa. They applied a simple interionic potential to the MD simulations. Later, Gour et al. [5] computed the phase transformation pressure (P_T) and elastic features of EuX materials by using three-body interaction potential (TBIP) in 2008. X. Wan and his friends [6] reported calculations with full potential linearized-muffin-tin-orbital (LMTO) method. They utilized the local spin density approximation (LSDA) and atomic Hubbard 1 (Hub1) combinations. Further, they reproduced known experimental results for bulk modulus, P_T and other magnetic properties in a numerical study in 2011. Afterwards, Varshney and colleagues [7] published pressure dependent mechanical characters of EuX compounds with the help of an effective interionic interaction potential. Meanwhile, Gupta and Singh [8] exerted charge-transfer potential (CTP) and modified-charge-transfer potential (MCTP) to EuX compounds in 2012. Gupta and Singh established a theoretical value for P_T and thermo elastic data of EuX compounds. In 2013, Kong et al. [9] surveyed the structural stabilities, elastic properties and charge transfers of EuX systems. They wielded ultrasoft pseudo potential scheme to their DFT calculations.

A couple of significant facts arise from the literature review [4-9] for high pressure elasticity and relevant values of EuO. The foremost point is the obtrusive disagreement between the stated results of typical cubic elastic constants (C_{11}, C_{12} *and* C_{44}) and bulk modulus (B). Even so, these results signify an analogy just for the P_T values. Another striking fact is the integrated scientific efforts conducting for the assessment of P_T alone. Moreover, to the best of our knowledge, there is not a detailed study yet in terms of elastic moduli *(B, E, and G)*

and elastic wave velocities (V_L and V_S) connected to the high pressure elasticity of EuO except the analysis of Ref [7]. As well, both dielectric constants (ε_0 and ε_∞) are also missing in Ref [7]. So, the main purpose of this work is to investigate the high pressure behavior and accompanying elastic constants of EuO in a more complementary way via the shell model potential framework by geometry optimization calculations.

In the next section, we will give a brief outline of computational details for shell model potentials and structure optimization. We will also perform a benchmark between our results, the experiments, and theoretical findings in the results and discussion section. Finally, we will summarize the present study in conclusion.

2. Computational details

Geometry optimization is a practical method for both MD and DFT to get a stable configuration for a molecule or periodic system. An optimization procedure involves the repeated sampling of the potential energy surface until the potential energy reaches a minimum where all forces on all atoms are zero.

Simple empirical potential models are the principal modeling intermediaries for oxides since they can produce successful and satisfying computing results. These potentials can well produce the defect energies, lattice constants, and elastic properties of oxides [10-12], fluorides [13-15] and other compounds [16-18]. The most potentials consists of Coulomb and pairwise short-range interactions with ionic polarization treated by the shell model of Dick and Overhauser [19]. The total energy is the sum of the Coulomb terms, short-range interactions, and the polarization of the ions for these potentials. The electron cloud of an ion i is simulated by a massless shell of charge of Y_i and the nucleus by a core of charge X_i, hence the total charge $q_i = X_i + Y_i$. The core and the shell of the ion i are coupled by a harmonic force with spring constant K_i. We assume the short-range pair interaction acts between the shells and for modeling them, we applied a typical Buckingham potential:

$$U_{ij}^{Buckingham} = A \exp\left(-\frac{r_{ij}}{\rho}\right) - \frac{C}{r_{ij}^6}$$

First term within the equation denotes the Born–Mayer whereas the second term stands for Van der Waals energies. Also, *A, ρ, C, Y,* and *K* are adjustable parameters for the fitting routine [20]. Lewis and Catlow [21] traced a series of potentials and distinct calculation methods for oxides by neglecting above attractive second term because of the small contribution of such terms to the short-range potentials including EuO. However, high experimental value of the static dielectric constant (ε_0= 26.5) of EuO suggests high polarization for this material. Thus, contrary to original conjecture [21], we also considered the effect of last term in this study.

All herein done geometry optimization calculations were performed with General Utility Lattice Program (GULP) code 4.0. during the present work [22,23]. GULP allows the least square fitting routine of calculated results to experimental observables existing in the literature. For fitting, our experimental observables were $C_{11}, C_{12}, and\ C_{44}$ and bulk modulus (B) as well as both dielectric constants.

The basic focus of a fitting is deriving potential parameters that can minimize the difference between optimized and experimental structures and properties [24]. So, it is desirable to optimize the concerned structure. The most customary optimization techniques are optimizing the related structures at constant pressure, in which all internal and cell variables are included or at constant volume, where the unit cell remains frozen. Hence, we applied a constant pressure optimization for EuO. We optimized the geometry of cells by the Newton–Raphson method based on the Hessian matrix calculated from the second derivatives. The Hessian matrix was recursively updated during optimization using the BFGS [25-28] algorithm through the fitting procedure. In addition, the potential parameters *A, ρ, C, and K* were the selected as variables where other parameters and oxygen-oxygen interaction kept same as in Ref. [21]. After setting the prerequisites for a conventional fitting [20] we devised multiple runs at zero Kelvin (0K) temperature and checked the pressure ranges starting from 0 GPa up to 50 GPa in the steps of 10 GPa.

3. Results and discussion

Tables 1-3 display the obtained data of present study with applied shell model potential parameters. Table 1 lists the assigned values for europium core, oxygen core, and oxygen shell which these values can maintain the charge neutrality of the europium oxide. Also, Table 2 denotes the Lewis and Catlow [21] parameters and obtained parameters after fitting. (A, ρ, C, and K were the fitting variables where cut-offs, charges and Eu shell interaction kept equivalent to the original parameters of the Lewis and Catlow [21]). To be able to attain a comparison, Table 3 summarizes the elaborated data of present, experimental and other calculated data (for 0K and 0GPa) with new potential parameters after fitting.

Table 1. Assigned values for europium core, oxygen core, and oxygen shell.

Species	Y(e)
Eu core	+2.000
O core	+0.869
O shell	-2.869

Table 2. Comparison of the original and present shell model potential parameters.

Buckingham Potential	**Lewis and Catlow [21]**	**Present**
	Eu core-O shell	
A (ev)	665.200	129.481
$\boldsymbol{\rho}$ (Å)	0.394	0.821
C (ev/Å^6)	0.100	0.462
Min. Cut-off (Å)	0.000	0.000
Max. Cut-off (Å)	10.00	10.00
	O shell-O shell	
A (ev)	22764	462646
$\boldsymbol{\rho}$ (Å)	0.149	0.276
C (ev/Å^6)	27.879	10147.4
Min. Cut-off (Å)	0.000	0.000
Max. Cut-off (Å)	12.00	12.00
	O (core-shell)	
K (ev/Å^2)	74.92	18.13

Table 3. Comparison of the previous and present data for EuO.

	Present	**Experiments**	**Others**
Lattice parameter, a_0 (Å)	5.140	5.141[(a)], 5.143[(a)]	3.63[(c)]
Density, d (g/cm^3)	8.207	8.197[(a)]	
P_T (GPa)	43	40[(b)]	36[(d)], 44[(e)], 49[(c)]
C_{11}	201	192[(a)]	177[(c)], 189[(f)], 251[(d)],
C_{12}	58.1	42.5[(a)]	43[(c)], 55[(d)], 62[(f)]
C_{44}	58.1	54.2[(a)]	54[(c)],52[(d)],78[(f)]
B (GPa)	106	107[(a)]	87[(c)]
G (GPa)	63.1	-	59[(c)],
E (GPa)	175	-	144[(c)],
V_S (km/s)	2.7	-	3.1[(g)]
V_L (km/s)	4.8	4.8[(a)]	4.8[(g)]
ε_0	26.4	26.5[(a)]	-
ε_∞	4.5	4.6[(a)]	-

[(a)]Ref [32], [(b)] Ref [33], [(c)] Ref [9], [(d)] Ref [5], [(e)] Ref [6], [(f)] Ref [34], [(g)] Ref [7]

From a crystallographic outlook, EuO compounds indicate a first-order phase transformation from a six-fold-coordinated B1 phase with space group $Fm\bar{3}m$ to eightfold-coordinated B2 phase with space group $Pm\bar{3}m$ at a critical phase transformation pressure (P_T) [8]. Fig. 1 depicts $P-V$ diagram of EuO for the entire pressure range applied during this study. Both $P-V$ or $P-T$ diagrams are frequently used for determining the equation of state (EOS) of materials with high pressure and/or at high temperature and contribute to thermodynamic property investigations. It is obvious from Fig.1 that volume of EuO decreases smoothly up to 43 GPa. At this pressure, the sharp decrease in volume originates from the structural changes associated with the $B1 \rightarrow B2$ first ordered phase transformation. The value of P_T with 43GPa shows a slight overestimation of the experiments within 7.5% and better than those obtained in former theoretical data (Table 3).

C_{11}, C_{12} *and* C_{44} describe the mechanical hardness of a material and needed for specifying the stability of the material. These elastic constants derived from the total energy calculations represent single crystal elastic properties [1,29]. On the other hand, Voigt-Reuss-Hill approximation is a confident scheme for polycrystalline materials [30]. To capture correct values of elastic constants and other connected parameters of EuO, we used the Voigt-Reuss-Hill scheme during our calculations.

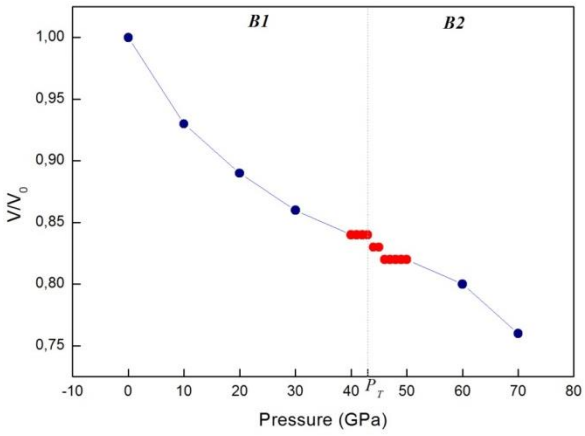

Fig. 1. P-V EOS of EuO up to 50 GPa.

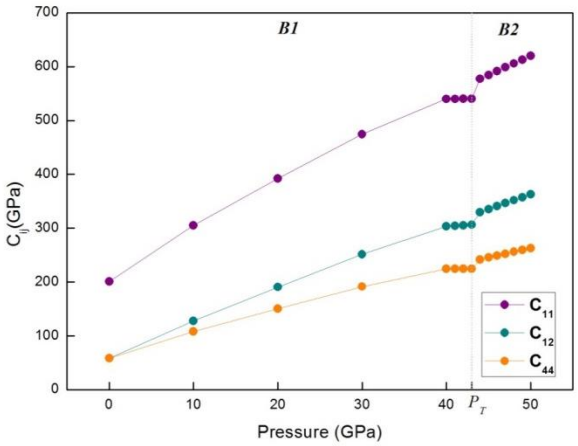

Fig. 2. Typical cubic elastic constants (C_{11}, C_{12} and C_{44}) of EuO under pressure at 0 K.

There is a little overestimation for C_{11} and our result is within 4.6% of experimental data where C_{12} exaggerate within 36.7% as in Table 3. Similar to C_{11}, C_{44} elastic constant deviates from the experiments within only 7.1%. Careful analysis of elastic constants C_{12} and C_{44} reveal an identical equality in Table 3, which this case holds well-known Cauchy condition as $C_{12} = C_{44}$ (in the absence of external pressure) for cubic crystals at 0K temperature under 0GPa pressure.

In addition to elastic constants, the bulk modulus (B) is the only elastic parameter of a material that reveals much information about the bonding strength. It is also a measure of the matters resistance to external deformation and occurs in many formulas describing diverse mechanical– physical characteristics [1,29].

According to Born structural stability, these constants must satisfy $C_{11} - C_{12} > 0$, $C_{11} > 0$, $C_{44} > 0$, $C_{11} + 2C_{12} > 0$ and cubic stability exemplary $C_{12} < B < C_{11}$ conditions [29,30]. As another result, calculated values of C_{11}, C_{12} and C_{44} elastic constants and B modulus well corroborate the both structural and cubic stability conditions for EuO.

Fig. 2 outlines the pressure dependence of the elastic constants between the 0GPa - 50GPa range obtained during this research. As seen in Fig. 2, the calculated values of elastic constants C_{11}, C_{12} and C_{44} are positive and exhibit a linear increment as a function of the increasing pressure. Besides, the increment of the elastic constant C_{11} is higher than the both elastic constants C_{12} and C_{44}. Physically, C_{11} explains the longitudinal elastic behavior whereas C_{12} and C_{44} portray the off-diagonal and shear elastic characteristic of cubic crystals because of shearing, respectively. So, a longitudinal strain produces a change in volume without a change in shape. This volume change is highly related to pressure, thus reflects a larger change in C_{11}. In contrast, a transverse strain or shearing causes a change in shape without a change in volume. Therefore, C_{12} and C_{44} are less sensitive to pressure when compared with C_{11}. These typical elastic constants have also an abrupt change at the phase transformation pressure 43 GPa.

Fig. 3 depicts the behavior of three elastic moduli ($B, G,$ and E) of EuO for the entire pressure range. By the way, shear modulus, (G) defines the resistance to shape change caused by a shearing force. Young's modulus (E) is the resistance to uniaxial tensions. These three elastic moduli ($B, G,$ and E) are principal parameters for determining the mechanical properties of materials [30]. From the common physical definition of bulk modulus $B = \Delta P / \Delta V$ it is expected an increment for B because of its direct proportion to applied pressure. Thus, in Fig.3 bulk modulus of EuO exemplify a straight increment in both $B1$ and $B2$ phases as expected. The other elastic moduli G and E strictly correlated with B are in similar trend as in Fig.4. Once more, $B, G,$ and E have an obvious decrease at $B1 \rightarrow B2$ phase transformation pressure. Further, our result for B only deviates within %0,9 from experiments (Table 3.). It is worth to note here that, no experimental data is available for G and E moduli of EuO. Anyway, we presented our results for G and E moduli in Table 3.Overall, the behavior in $B, G,$ and E curves is also in harmony within the former results of moderating pressures in materials.

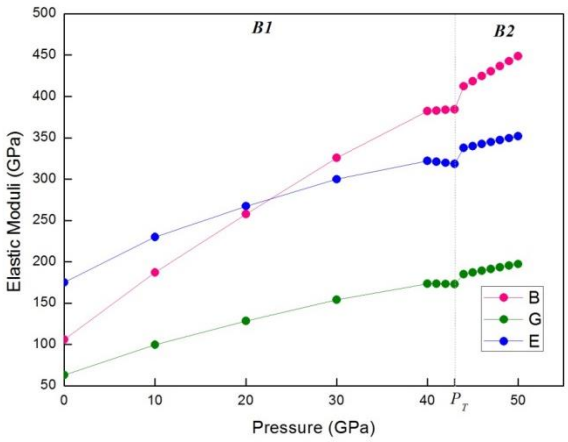

Fig. 3. Bulk modulus, shear modulus and Young's modulus of EuO under pressure at 0 K.

Low temperature acoustic modes trigger vibrational excitations in solids. Depending on this case, two typical elastic waves, namely, the longitudinal wave and shear wave arise [29]. Therefore, V_L and V_S stand for these wave velocities, respectively. The values of both velocities are given in Table 3. and they are identical with experiments. Also, Fig.4 illustrates the high pressure behavior of V_L and V_S of EuO. As in the above mentioned other parameters both velocities exhibit uniform increment tendency with the increasing pressure in $B1\ and\ B2$ phases and a dramatic decrease at 43 GPa accompanying the $B1 \rightarrow B2$ phase transformation.

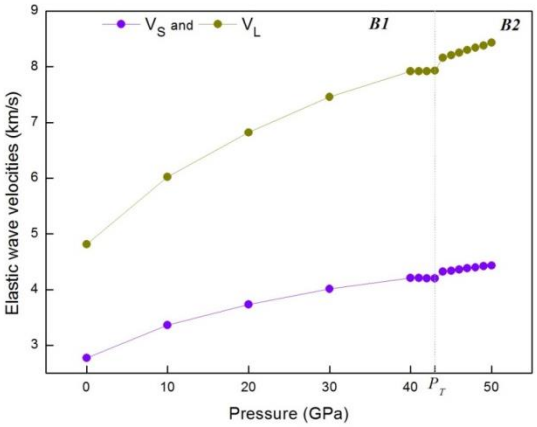

Fig. 4. High pressure behavior of V_L and V_S of EuO at 0 K.

The dielectric constants of materials are fundamental parameters for device design in nearly all fields of modern electronics and responsible for the behavior of charge carriers, dopants, defects, impurities, insulators and semiconductors [31]. The plots of the dielectric constants behavior for EuO under considered pressure range can be seen in Fig. 5. Both dielectric constants ($\varepsilon_0\ and\ \varepsilon_\infty$) increase with increasing pressure for both phases. Moreover, ε_0 deviates within -0,37% from experiments, whereas the deviation of ε_∞ is 2.1%. (Table 3.) As it is also clear from Fig. 5, obtained results for ε_0 indicates a decrease at $B1 \rightarrow B2$ phase transformation pressure, while ε_∞ keep its sluggish increasing behavior under pressure.

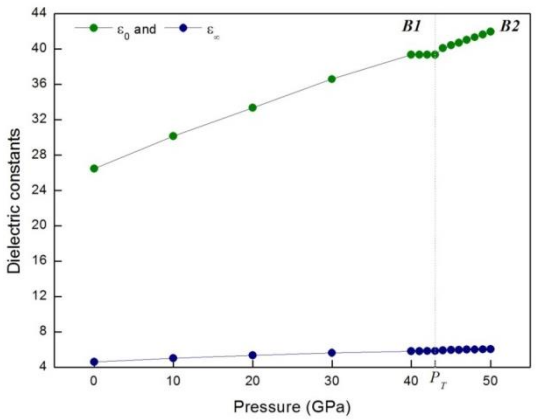

Fig. 5. High pressure behavior of $\varepsilon_0\ and\ \varepsilon_\infty$ dielectric constants of EuO at 0 K.

Of the above mentioned findings, all considered parameters during the present study confirm each other and point out a $B1 \rightarrow B2$ phase transformation at 43 GPa for EuO under pressure .

Overall, fitted potential parameters produce sensible results which are consistent with former available data. Especially, obtained data of crystal density, bulk modulus and formerly missing dielectric constants are almost identical with experiments and better than those of some early attempts (Table 3).

4. Conclusion

In contrats to existing literature methods and applied potentials, this is the first study within the shell model potential framework for structural, elastic, mechanical and related properties of EuO under pressure. It should be also noted that significance of this work is not only calculating the high pressure phase transformation and cubic elastic constants of EuO, but also predicting the pressure dependence of typical cubic elastic constants bulk modulus, shear modulus, Young's modulus, the longitudinal and shear wave velocities and *previously missing dielectric constants*.

It can be emphasized that our results are reasonable with both experiments and early theoretical findings and they can be used in the future works of this prominent material.

References

[1] E. Güler, M. Güler, Adv. Mater. Sci. Eng. **2013** Article ID 525673 (2013).
[2] H. Wang, C. Schuster, U. Schwingenschlögl Chem. Phys. Lett **524**, 68 (2012).
[3] U. K. Sakalle, P. K. Jha, S. P. Sanyal , Bull. Mater. Sci **23**, 233 (2000).
[4] A. K. M. A. Islam, Shahdatullah M S 1994 International Center for Theoretical Physics IC/94/351.
[5] A. Gour, S. Singh, R. K. Singh, M. Singh, Pramana J Phys **71**, 181–6 (2008).
[6] X. Wan, J. Dong, S. Y. Savrasov, Phys. Rev. B **83**, 205201 (2011).
[7] D. Varshney, S. Shriya, M. Varshney, R. Khenata, Comp. Mater. Sci. **61**, 158–79 (2012).
[8] D. C. Gupta, K. C. Singh, J. Mol.Modeling **18**, 3003–12 (2012).
[9] B. Kong, Z.-W. Zhou, X.-W. Sun, L. Zhang, R.-F. Ling-Hu, Acta Phys. Pol. A **123**, 720–7 (2013).
[10] M. Nadeem, M. J. Akhtar, R. Shaheen, M. N. Haque, J. Mater. Sci. Technol. **17**, 638-42 (2001).
[11] S. Dai, M. L. Dunn, H. S. Park, Nanotechnology **21**, 445707 (2010).
[12] Z. J. Liu, X. W. Sun, Q. F. Chen, L. C. Cai, X. M. Tan, X. D. Yang, Phys. Lett. A **353**, 221–5.
[13] M. E. G. Valerio, R. A. Jackson, J. F. de Lima, J. Phys.: Condens. Matter. **12**, 7727–34 (2000).

[14] R. A. Jackson, T. E. Littleford, G. E. Newby, D. F. Plant, IOP Conf. Ser. Materials Science and Engineering **15**, 012048 (2010).
[15] R. A. Jackson, E. M. Maddock, M. E. Valerio, G, IOP Conf. Ser.Materials Science and Engineering **15**, 012014 (2010).
[16] A. Chroneos, I. L. Goulatis, R. V. Vovk, Acta. Chim. Slov. **54**, 179 (2007).
[17] C. Yan, T. U. Ya- jing, Z. Zhao-yi, G. O. U. Qing-quan, Commun. Theor. Phys. **50**, 1443-8 (2008).
[18] P. E. Ngoepe et al. S .Afr. J. Sci. **101**, 480-3 (2005).
[19] B. G. Dick, A. W. Overhauser, Phys. Rev. **112**, 90 (1958).
[20] J. D. Gale, Phil. Mag. B **73** 3–19 (2006).
[21] G. V. Lewis, C. R. A. Catlow J.Phys.C: Solid State Phys. **18**, 1149–61 (1985).
[22] J. D. Gale, J. Chem. Soc. Faraday **93**, 629 (1997).
[23] J. D. Gale, A. L. Rohl, Mol. Smilulat. **29**, 291 (2003).
[24] J. D. Gale, Z. Kristallogr. **220**, 552–4 (2005).
[25] G. C. Broyden, J. Inst. Math. Appl. **6**, 76 (1970).
[26] R. Fletcher, Comput. J. **13**, 317 (1970).
[27] D. Goldfarb, Math. Comput. **24**, 23 (1970).
[28] D. F. Shanno, Math. Comput. **24**, 647 (1970).
[29] M. Güler, E. Güler Chin. Phys. Lett. **30**, 056201 (2013).
[30] E. Güler and M. Güler, Mat. Res. [online]. ahead of print, pp. 0. Epub Aug 15, (2014). doi: 10.1590/1516-1439.272414
[31] E.Güler and M. Güler, Chin. J. Phys. **52**, 1625 (2014).
[32] Landolt-Börnstein: Numerical Data and Functional Relationships in Science and Technology- New Series, Subvolume 17g, 1984, Springer, New York.
[33] A. Jayaraman, A. K. Singh, A. Chatterjee, S. U. Devi, Phys. Rev. B, **9**, 2513 (1974).
[34] J. M. An, S. V. Barabash, V. Ozolins, M. van Schilfgaarde, K. D. Belashchenko, Phys. Rev. B **83**, 064105 (2011).

*Corresponding author: mlkgnr@gmail.com